Uncertainties and their interaction in flood hazard assessment with climate change

Hadush Meresa[1], Conor Murphy[1], Rowan Fealy[1], Saeed Golian[1]

[1]Irish Climate Analysis and Research UnitS (ICARUS), Dept. of Geography, Maynooth University, Maynooth, Ireland.

Correspondence to: Hadush Meresa (Hadush.Meresa@mu.ie)

Abstract

The assessment of future impacts of climate change is associated with a cascade of uncertainty linked to the modelling chain
10 employed in assessing local scale changes. Understanding and quantifying this cascade is essential to developing effective adaptation actions. We evaluate and quantify uncertainties in future flood quantiles associated with climate change for four catchments, incorporating within our modelling chain uncertainties associated with 12 Global Climate Models contained in the Coupled Model Intercomparison Project Phase 6, five different bias correction approaches, hydrological model parameter uncertainty and use of three different extreme value distributions for flood frequency analysis. Results indicate increased flood
15 hazard in all catchments for different Shared Socioeconomic Pathways (SSPs), with changes in flooding consistent with changes in annual maximum precipitation. We use additive chains and analysis of variance (ANOVA) to quantify and decompose uncertainties and their interactions in estimating selected flood quantiles for each catchment. We find that not only do the contributions of different sources of uncertainty vary by catchment, but that the dominant sources of uncertainty can be very different on a catchment by catchment basis. While uncertainties in future projections are widely assumed to be dominated
20 by the ensemble of climate models used, we find that in one of our catchments uncertainties associated with bias correction methods dominate, while in another uncertainty associated with use of different extreme value distributions outweigh the uncertainty associated with the ensemble of climate models. These findings highlight the inability to generalise a priori about the importance of different components of the cascade of uncertainty in future flood hazard at the catchment scale. Moreover, we find that the interaction of components of the modelling chain employed are substantial (>20 percent of overall uncertainty
25 in two catchments). While our sample is small, there is evidence that the dominant components of the cascade of uncertainty may be linked to catchment characteristics and rainfall-runoff processes. Future work that seeks to further explore the characteristics of the uncertainty cascade as they relate to catchment characteristics may provide insight into a-priori identifying the key components of modelling chains to be targeted in climate change impact assessments.

30 **Keywords:** modelling, flood, climate change, uncertainty, impact, bias correction, GLUE, GR4J

1 Introduction

Climate change is likely to increasingly affect hydrological regimes and flood hazards over coming decades. Considerable changes in atmospheric temperature, precipitation, humidity, and circulation are expected, which may result in increasing extreme events, including floods (IPCC, 2013). According to Rojas et al. (2013), flood frequency in Europe will increase due to climate change, with significant socio-economic implications for the region. Blöschl et al. (2017) and Blöschl et al. (2019) conclude that the timing and magnitude of European floods have shifted due to climate change and its consequences are not uniform across the region, with north-western Europe experiencing earlier and higher flood peaks. Modelling and understanding of catchment scale flood hazard projections is therefore an important endeavour for informing adaptation strategies.

Climate change impact assessment is subject to considerable uncertainties (Wilby and Dessai, 2010; Smith et al., 2018); Blöschl et al. (2019) recently highlighted uncertainty in hydrology as one of the 25 challenges in hydrological science. Traditional or top-down climate change impact assessments typically follow a modelling chain where output from Global Climate Models (GCMs), forced with scenarios of future greenhouse ~~estimates of future greenhouse~~ gas concentrations, are extracted, and scaled to represent a study catchment. Hydrological models, calibrated for current conditions, are then forced with these GCM outputs to create discharge series spanning multiple decades into the future. When assessing flood hazard, extreme value distributions are typically fitted to samples of extreme events (e.g. annual maximum flood series) representing current and future climates to evaluate changes in the characteristics of flooding. This modelling chain is replete with uncertainties that propagate and interact, resulting in potential large ranges in projected change at the catchment scale (e.g. Meresa, 2019) that can impede decision making (Smith et al., 2018).

Numerous studies have attempted to quantify the uncertainties in future climate change impacts due to the use of different climate models (e.g Knutti & Sedláček, 2013), natural variability (e.g. ~~(~~Giuntoli et al., 2018; Hughes et al., 2011), bias correction techniques (e.g. Kay et al., 2009; Saini et al., 2015; Soriano et al., 2019), downscaling approaches (e.g. Fowler et al., 2007; Gutmann et al., 2014), hydrological modelling uncertainties (e.g. Wilby & Harris, 2006; Bastola et al., 2011; Addor et al., 2014; Meresa & Romanowicz, 2017; Broderick et al., 2019) and the application of different extreme value distributions for flood hazard estimation (e.g. Meresa & Romanowicz, 2017; Lawrence, 2020). Findings from such studies confirm that the dominant source of uncertainty varies across studies. For example, Jobst et al. (2018) concluded that the GCM structure is the dominant contributor followed by emission scenario, bias correction, and hydrological model structure in New Zealand catchments. Peleg et al. (2015) found that the hydrological regimes are highly sensitive to changes in convective precipitation in eastern Mediterranean catchments. Gosling et al. (2011) evaluated seasonal flow changes in UK catchments and found greater uncertainty in future estimates due to climate models than hydrological models. In Norwegian catchments Lawrence (2020) highlighted that climate models and frequency models are dominant sources of uncertainty in future flood projections.

Therefore, the key components of the uncertainty cascade and their contributions tend to vary depending on the region, precipitation type, and catchment.

Recognition of the uncertainties inherent in future climate change impacts has also given rise to novel approaches to decision-making that embrace uncertainties (e.g. Wilby & Murphy, 2019; Clark et al., 2016). Rather than aiming to derive precise assessments of future risk, such approaches aim to stress test and evaluate adaptation options, in static or dynamic ways (Mazzorana et al., 2012), to identify actions that are functional across a range of plausible future conditions, rather than optimised to a certain outcome (e.g. structured decision making (SDM), robust decision making, decision scaling, adaptation pathways). Shepherd et al., (2018) recommend a storyline approach for navigating uncertainty, whereby examination of recent, notable extremes and the development of plausible narratives of change in their drivers enables novel assessment of future changes, placing emphasis on physical processes. Each of these approaches require the cascade of uncertainty to be evaluated or navigated in ways that can better inform adaptation. For example, Broderick et al. (2019) employ a scenario neutral framework (Prudhomme et al., 2011) to evaluate design allowances for flood defences taking into account uncertainties derived from a large climate model ensemble, natural variability and hydrological models.

Whether employing traditional impact led or novel decision centric approaches, it is critical that key components of the cascade of uncertainty are adequately included. Research over the past two decades clearly shows that methodological choices made in assessing future climate change fundamentally impact on the portrayal of climate risk (Clark et al., 2016; Melsen et al., 2019). Top-down approaches must a-priori decide on the components of the modelling chain to include. Including all relevant components is typically a very resource expensive task (Smith et al., 2018) and it may not be apparent at the outset which components of the ~~aggregated~~ uncertainty cascade~~uncertainty modelling chain~~ to include for specific catchments. For bottom up approaches, such as the scenario neutral method (Broderick et al., 2019), the modeller is forced to choose which aspects of uncertainty to ~~prioritise~~ include in assessing sensitivity to future changes. Again, this may not be apparent from the outset. It is widely acknowledged that climate models exhibit biases in their outputs (Krinner & Flanner, 2018; Giorgi & Gao, 2018), with numerous studies highlighting the need to post-process climate model output before use in simulating hydrological response (Ehret et al., 2012; Teng et al., 2012; Osuch et al., 2017; Meresa & Romanowicz, 2017). Dobler et al. (2012) suggest that the dominant components of the modelling chain may further vary depending on which part of the flow regime (low, mean, high flows) is of interest. They highlight, for example, that the importance of bias correction approaches to the overall uncertainty in hydrological response increases for high flows. However, there is still no consensus on which bias correction techniques are most effective, nor in how bias correction techniques can modify future climate change signals. For instance, Teutschbein & Seibert (2013) and Yang et al. (2010) showed distribution mapping based on theoretical distributions outperforms other bias correction methods. Similarly, Berg et al. (2012) and Chen et al. (2013) show that theoretical distribution mapping performs similar to, or marginally better than, empirical quantile mapping. On the contrary,

Gudmundsson et al. (2012), Gutjahr & Heinemann, (2013) and Lafon et al. (2013), show that empirical quantile mapping demonstrates higher skill than theoretical distribution mapping in systematically correcting precipitation.

100 Moreover, deep uncertainty can arise by virtue of the ad-hoc ways in which components of possible modelling chains are assembled and characterised within the overall modelling framework adopted (Wilby and Murphy 2019). Yet there are currently no established ways of sampling from the hierarchy of models used to evaluate impacts of climate change (Clark et al., 2016). Therefore, an important step in better integrating future climate risk into decision-making is quantifying and partitioning the contribution of different components of uncertainty and their interactions to help scientists and decision makers
105 better navigate the cascade of uncertainty by identifying contributing sources that should be more fully explored (Smith et al., 2018). In this regard ANOVA (ANalysis Of Variance) based techniques, which can be used to decompose sources of uncertainty and their interaction, offer considerable utility (e.g. Kay et al., 2009; Vetter et al., 2016; Hattermann et al., 2018; Meresa, 2020). In this study, we explore uncertainties in future flood hazard for four catchments, representative of different flood response types, in Ireland and employ additive chains and variance decomposition to quantify and examine the
110 contribution of various sources of uncertainty, together with their interaction, to the overall uncertainty in flood hazard projections. In doing so we place emphasis on evaluating the uncertainties derived from; i) climate models in the newly available Coupled Model Inter-comparison Project Phase 6 (CMIP6) ensemble (Wyser et al., 2019); ii) widely used bias correction techniques; iii) hydrological model parameter uncertainty, and iv) the use of different extreme value distributions. The remainder of the paper is organised as follows; Section 2 outlines the study design and data/methods employed, Section 3
115 presents key results, exploring uncertainties for key steps in the modelling chain examined, together with their contributions and interactions to the full range of projected change in flood risk. Section 4 provides a discussion of key insights, limitations and future directions before drawing main conclusions in Section 5.

2 Models and Study Design

Our study design is illustrated in Figure 1. We quantify uncertainties and their interaction in projected flood hazards using 12
120 ~~Global~~ Climate Models (~~G~~CMs) contained in the Coupled Model Inter-comparison Project Phase 6 (CMIP6) ensemble (https://esgf-node.llnl.gov/search/cmip6/), forced using three Shared Socioeconomic Pathways (SSP) scenarios. We use five bias correction techniques (Change factor (CF), Double Gamma Distribution Quantile (DGQM), Birnbaum distribution Quantile mapping (BQM), Single Gamma Distribution Quantile (SGQM), and Empirical Quantile (EQM)) to post-process climate model outputs (daily precipitation and air temperature time series). The daily bias corrected precipitation and
125 temperature data are used as input to the Génie Rural à 4 paramètres Journalier (GR4J) hydrological model (Perrin et al., 2003). The Generalized Likelihood Uncertainty Estimation (GLUE) technique is used to quantify GR4J parameter uncertainty. In assessing future flood hazard the sensitivity of results to different extreme value distributions is examined. In addition to evaluating each source of uncertainty independently, we use variance decomposition to quantify the contribution of each

methodological choice and their interactions to the overall uncertainty in assessing flood risk. The climate change impact is evaluated based on relative future changes in the magnitude of floods for the 2020s (2010-2039), 2050s (2040-2069) and 2080s (2070-2099) with respect to the reference period (1976-2005). The following sections provide further details on the study catchments and each stage of the modelling chain employed.

2.1 Study catchments and hydro-climate datasets

Simulations are undertaken for four catchments (Boyne, Blackwater, Newport and Slaney), representing different flood response types across the Ireland (Broderick et al., 2019). Their location, together with a summary of hydro-climatic conditions for each catchment is summarized in Table 1 and Figure 2. Catchment area ranges from 146 km^2 (Newport) to 2447 km^2 (Boyne), while mean elevation ranges from 56 m (Newport) to 112 m (Blackwater). For each catchment we use gridded (1×1 km) daily precipitation and temperature data (Walsh, 2012) area averaged for the period 1976-2005 to provide a single representative baseline series for each catchment. Daily potential evapotranspiration is derived using air temperature and elevation following the method of Hamon (1964). This approach is favored over less parsimonious but more physically based methods (e.g. Penman-Monteith), which have greater data input requirements (e.g. wind speed, humidity) not available for all study catchments. Daily discharge data for each catchment was obtained from the Office of Public Works (OPW) (**http://www.epa.ie/hydronet/**).

2.2 Climate Projections and Bias Correction

Daily precipitation (pr) and air temperature (tas) time series for the period 1971-2100 were extracted for 12 members of the CMIP6 ensemble (https://esgf-node.llnl.gov/search/cmip6/) forced by each of three Shared Socioeconomic Pathway (SSP) (SSP126, SSP370 and SSP585) scenarios (see Table 2 for details). For each catchment daily precipitation and air temperature were extracted from the closest land based GCM grid overlying the catchment centroid. We employ five commonly used techniques to bias correct raw climate model output and to examine the contribution of the selected bias correction methods to the total uncertainty in future flood hazard.

2.2.1 Change factor /delta change (CF)

The change factor technique applies multiplicative (for precipitation) and/or additive (for temperature) procedures for correcting raw model output. This involves correcting simulated daily precipitation ($P_{fut,corr}$) by multiplying the ratio of observed precipitation (P_{obs}) and reference precipitation simulation ($P_{ref,raw}$) to future simulations of raw climate model precipitation ($P_{fur,raw}$). For correcting future air temperature ($T_{fut,corr}$), the difference in observed air temperature (T_{obs}) and simulated temperature in the reference period ($T_{ref,raw}$) is added to raw climate output ($T_{fur,raw}$).

$$P_{fut,corr} = P_{fur,raw} * \frac{P_{obs}}{P_{ref,raw}} \tag{1}$$

$$T_{fut,corr} = T_{fur,raw} + (T_{obs} - T_{ref,raw}) \tag{2}$$

2.2.2 Empirical quantile mapping (EQM)

Empirical quantile mapping is based on pair-wise comparison between the empirical cumulative density functions (ecdf) of observed and simulated daily precipitation time series during the reference period (1976-2005). This is a purely empirical approach with direct matching of the histogram of the observed precipitation to the future period. Future precipitation and temperature are corrected using the inverse of the ecdf ($ecdf^{-1}$) and fitted ecdf $ecdf_{hst,m}$.

$$P^{cor}_{hst,m} = (ecdf^{-1}_{obs,m}(ecdf_{hst,m}(P_{hst,m}))) \tag{3}$$

$$T^{cor}_{hst,m} = (ecdf^{-1}_{obs,m}(ecdf_{hst,m}(T_{hst,m}))) \tag{4}$$

The non-parametric quantile matching was performed first in the reference period (m, modeling period) using an exponential transfer function assumption. Then the calibrated coefficients were used to correct the future daily precipitation and air temperature.

2.2.3 Distribution Quantile Mapping (DQM)

Distribution quantile mapping is a distribution parameter dependant bias correction technique. The parameters are extracted by fitting Gamma distribution to observed and simulated time series data, and matching its corresponding quantiles from the observed and raw climate model output in the reference period (1976-2005) (Piani et al., 2010). We applied two types of DQM to correct climate biases: Single Gamma Distribution Quantile Mapping (SGDQM) and Double Gamma Distribution Quantile Mapping (DGDQM), together with the Birnbaum-Sanders distribution method (BSM) (Marzena Osuch et al., 2016). These methods also allow for any excess in the number of dry, drizzle and wet days to be considered and corrected. In the case of SGQM, the first step is fitting a Gamma distribution to the upper 75 % of daily observed and raw climate output precipitation distribution. Whereas in the DGDQM, the Gamma distribution is fitted to both the upper ≥ 75 % and to the lower < 75 % of the daily observed and raw climate output precipitation in the reference period (1976-2005). In both cases, non-rain days were removed and only wet days were considered. Similarly, BSM used the Birnbaum-Sanders distribution to transfer the precipitation quantile from the observed time series to raw output of the GCMs in the reference period.

$$P_{corr} = F^{-1}_{dg}(F_{dg}(P_{raw}(t), \alpha_{raw}, \beta_{raw}), \alpha_{Obs}, \beta_{Obs}) \tag{5}$$

$$P_{corr} = F_{db}^{-1}(F_{db}(P_{raw}(t), \alpha_{raw}, \beta_{raw}), \alpha_{Obs}, \beta_{Obs}) \tag{6}$$

190

$$T_{corr} = F_{db}^{-1}(F_{db}(T_{raw}(t), \alpha_{raw}, \beta_{raw}), \alpha_{Obs}, \beta_{Obs}) \tag{7}$$

$$T_{corr} = F_{dn}^{-1}(F_{dn}(T_{raw}(t), \alpha_{raw}, \beta_{raw}), \alpha_{Obs}, \beta_{Obs}) \tag{8}$$

195   Where P_{corr} and T_{corr} are the bias corrected daily precipitation and temperature, respectively. Likewise, $P_{raw}(t)$ and $T_{raw}(t)$ represent for raw climate model output for precipitation and temperature. The raw climate output inverse cumulative density (CDF) is symbolized by F_{dg}^{-1}, F_{db}^{-1}, and F_{dn}^{-1} for precipitation and temperature, respectively. The dn, db and dg subscripts represent the normal (for temperature), Birnbaum-Sanders (for both precipitation and temperature) and Gamma (for precipitation) distributions, respectively. The Gamma (for precipitation) and Birnbaum-Sanders distributions have two

200   parameters – the shape and scale parameters which are symbolised by α and β, and the normal (for temperature) distribution, with mean and standard deviation represented by μ and σ, respectively.

2.3 Bias correction performance evaluation

The performance of the selected bias correction techniques was evaluated using four statistical measures: Pearson Correlation (RR), Mean Absolute Error (MAE), Root Mean Square Error (RMSE) and Percent Bias (PBIAS). Evaluation was performed

205   by comparing the ability of each approach to capture observed precipitation and temperature.

$$RR = \frac{\sum(P_S - \overline{P_S}) * (P_C - \overline{P_C})}{\sqrt{\sum(P_S - \overline{P_S})^2 * \sum(P_C - \overline{P_C})^2}} \tag{9}$$

$$MAE = \frac{\sum_{i=1}^{n}|P_S - P_C|}{N} \tag{10}$$

210

$$PBIAS = \frac{\sum_{i=1}^{n}|P_S - P_C|}{\sum_{i=1}^{n} P_S} \tag{11}$$

$$RMSE = [\frac{\sum_{i=1}^{n}|P_S - P_C|^2}{N}]^{0.5} \tag{12}$$

215   Where Ps and Pc are observed and corrected precipitation, respectively, $\overline{P_C}$ is the mean of corrected precipitation, $\overline{P_S}$ the mean of observed precipitation and N is the number of observations.

2.4 Hydrological modelling

The GR4J model (Perrin et al., 2003) is a parsimonious four parameter, lumped conceptual rainfall-runoff model that has been widely applied in different hydro-climate conditions (Meresa & Gatachew, 2019; Meresa et al., 2017; He et al., 2018). The
220 model is particularly suited to climate change impact studies given its parsimonious structure. GR4J simulates streamflow using precipitation, temperature and potential evapotranspiration (Perrin et al., 2003) and has previously been successfully used in Ireland to assess climate change impacts (Broderick et al. 2016; Broderick et al., 2019), river flow reconstructions (O'Connor et al., 2020) and seasonal hydrological forecasting (Donegan et al., 2020). Broderick et al. (2019) highlight the good performance of GR4J in capturing a range of hydrological signatures across diverse Irish catchments (Broderick et al.,
225 2019). The model has two consecutive stores: one related to runoff production and the other to runoff routing. Detailed information about the model structure is given in Perrin et al. (2003). The upper and lower limits of the four model parameters are listed in Supplementary Table S1. The model was calibrated and validated using observations over the period 1976-2005. The first four years were used as a model warmup to stabilise the initial states of the hydrological parameters. Calibration was undertaken from 1981-1999 and validation from 2000-2005. The Nash Sutcliffe Efficiency (NSE) objective function was used
230 to evaluate the model performance and to identify behavioural parameter sets (Nash and Sutcliffe, 1970). NSE is defined as:

$$NSE = 1 - \frac{\sum_{t=1}^{j}(Q_{o,t}-Q_{m,t})^2}{\sum_{t=1}^{j}(Q_{o,t}-\bar{Q}_o)^2} \qquad (13)$$

where $Q_{o,t}$ and $Q_{m,t}$ are observed and simulated flow at time t, Q_o is the mean observed flow and j is the length of the jth time series. The ability of hydrological model simulations to replicate the observations was further evaluated by deriving the proportion of extreme high flows inside the 95% confidence intervals (PCI). This is helpful for identifying a fixed NSE
235 threshold for differentiating between behavioural and non-behavioural simulations (Li et al., 2011; Xu, 2014).

The Generalized Likelihood Uncertainty Estimation (GLUE) approach is widely applied to quantify hydrological model parameter uncertainty (Beven & Binley, 1992). GLUE is an informal statistical approach that uses Monte Carlo (MC) simulation to generate many possible hydrological parameter sets from specific ranges. The choice of the number of samples is somewhat subjective with studies typically employing a few thousand to tens of thousands of hydrological model parameter
240 set samples to simulate river flow (Zheng and Bennett, 2002). In applying GLUE, we randomly generated a large number of parameter sets (30,000) using a uniform distribution constrained by the acceptable ranges of each GR4J parameter. Behavioural parameter sets were identified based on NSE (Equation 13) scores >0.50.

2.5 Flood frequency analysis

Numerous extreme value distributions can be deployed to estimate the frequencies of high flows. For example, the Log-Pearson
245 III distribution is very popular in the USA and Australia for infrastructure design (Griffis & Stedinger, 2007), the General Extreme Value and Pearson Type III distributions are widely used in Europe (Madsen et al., 2013), while the Wakeby and Log-Normal distributions have been frequently used in Asia (Chen et al., 2012). However, a single distribution model may not

be able to capture the entire temporal and spatial variability of hydrological extremes. Therefore, we employ three common distribution types (LN, Log-logistic and GEV) with Maximum Likelihood parameter estimator (MLE) for flood frequency curve development. MLE estimates the distribution parameters by optimising the likelihood function of the cumulative probability distribution density, and its reliability is evaluated using the standard error of the estimated parameters. These distributions were fitted to the annual maximum daily peak flows in each study catchment. In Equations 14 - 16, the respective probability density function (PDF) of each distribution is presented. The Log-Normal and Log-logistic models have two parameters, while the GEV distribution has three parameters.

Log-Normal (LN) $\qquad f(x) = \dfrac{\exp\left(-\frac{1}{2}\left(\frac{lnx-\mu}{\sigma}\right)^2\right)}{x\sigma\sqrt{2\pi}} \qquad \sigma, \mu\ (\sigma{>}0)$ $\qquad\qquad$ (14)

Log Logistic (LogL) $\qquad f(x) = \dfrac{\mu\left(\frac{x}{\sigma}\right)^{\mu-1}}{\sigma\left[1+\left(\frac{x}{\sigma}\right)^{\mu}\right]^2}$ $\qquad\qquad\qquad\qquad\qquad\qquad$ (15)

GEV $\qquad f(x) = \begin{cases} \frac{1}{\sigma}\exp\left(-(1+k(\frac{x-\mu}{\sigma}))^{\wedge-\frac{1}{k}}\right)\left(1+k(\frac{x-\mu}{\sigma})\right)^{-1-\frac{1}{k}} & k \neq 0 \\ \frac{1}{\sigma}\exp\left(-(\frac{x-\mu}{\sigma}) - exp(-((x-\mu)/\sigma))\right) & k = o \end{cases}$ $\quad$ K, σ, μ ($\sigma{>}0$) (16)

Where, σ is the scale, μ is location and k is the shape parameter.

2.6 Uncertainty estimation and decomposition

We used two approaches to uncertainty analysis in future flood hazard. First is the additive chain approach which is similar to sensitivity analysis. whereby the main goal is to assess components of the modelling chain independently (one-at-the-time). Second, we used ANOVA to separate the variance contribution of each component of the modelling chain and their interaction. Unlike the former (sensitivity approach), it helps us to understand the interaction of factors and their main variables using their total variance values.

2.6.1 Additive chain approach

We examine the relative contribution of four key components of the modelling chain to the projected uncertainty in future flood hazard. These are climate models (CM), bias correction techniques (BC), hydrological model parameters (HP) and flood frequency distribution models (FF). We only use a single SSP scenario (here SSP370) in our evaluation of the uncertainty cascade, with the assumption that different studies will be interested in quantifying flood hazard for different emissions outcomes separately.

Overall uncertainty is estimated based on the additive chain method, while decomposition of the contribution of different sources of uncertainty and their interactions is evaluated using ANOVA. The uncertainty in future flood hazard can be defined as the total uncertainty resulting from the components (s) of the modelling chain considered – here four components *s1* to *s4* (CM, BC, HP and FF). Initially we define the cumulative uncertainty for each component (s) of the modelling chain denoted by $U^{cum}(X_1 \ldots X_s)$ and its respective conditional probability as $U(q_{x\ s+1\ldots\ldots xs})$. The uncertainty in our modelling chain is characterized as the total variance in the flood quantile generated from each of the four components evaluated, with total uncertainty defined as;

$$U^{cum}(x_1, \ldots, x_s) = \frac{1}{\pi_{j=s+1}^{nj}} \sum_{x_{s+1} \epsilon x_{s+1}} \cdots \sum_{x_s \epsilon x_s} U(q_{x\ s+1\ldots\ldots xs}) \tag{17}$$

$U(q_{x\ s+1\ldots\ldots xs})$ stands for respective cumulative probability of each output quantiles. This uncertainty quantification method keeps summing as the number of components (s) of the modelling chain increases. Therefore, the uncertainty of a particular step along the modelling chain e.g. s=4, denoted by $U^{cum}(X_{4s})$, can be described as:

$$U^{cum}(X_{s4}) = U^{cum}(X_{s4,\ldots,X_s}) - U^{cum}(X_{s3,\ldots,X_{s-1}}) \qquad \text{in general} \qquad U^{cum}(X_s) = U^{cum}(X_{s-1}) - U^{cum}(X_{s-2}) \tag{18}$$

Note that uncertainty of each component of the chain is a magnitude of contribution to the total uncertainty so that the sum of uncertainties of individual sources is always equal to the cumulated cumulative uncertainty $U^{cum}(X_1, \ldots, X_s)$. Whereas, eEquation 18 was used to get the individual component from the total uncertainty.

2.6.2 ANOVA approach

Unlike single chain based additive approaches to uncertainty estimation, ANOVA can decompose the aggregated source of uncertainty into individual components and their interaction using specific extreme flow indices (Meresa & Romanowicz, 2017) and in mean runoff projections (Bosshard et al., 2013). We develop a hypothesis test using an ANOVA model that can identify the effect of each component (CM, BC, HP, FF) in the model chain to the total variance of the extreme index (Y). According to n-way ANOVA principles, the model splits the total sum of squares (SST) into the sum of squares (SS) of the main variables and their interactions as follows:

$$SST = \sum_{i=1}^{NCM=12} \sum_{j=1}^{NBC=5} \sum_{k=1}^{NHP=300} \sum_{l=1}^{NFF=3} (Y_{ijkl} - \bar{Y})^2 \tag{19}$$

Where Y_{ijkl} is estimated flood magnitude considering i=12 climate models, j=5 bias correction methods, k=300 hydrological parameter sets, l=3 extreme frequency distributions, and $\bar{Y}$ is the mean of all variables. SST is the grand square deviation of

the main and interacting variables. Further, the deviation in SST is split into individual and interacting components to explore
their effect on the aggregated extreme flood frequency indices as follows:

$$SST = SS_{CM} + SS_{BC} + SS_{HP} + SS_{FF} + SS_{CMBC} + SS_{CMHP} + SS_{CMFF} + SS_{BCHP} + SS_{BCFF} + SS_{HPFF} \quad (20)$$

where SS_{CM} is the sum of standard errors of climate models, SS_{BC} is the sum of standard errors of bias correction methods, SS_{HP} the sum of standard errors of hydrological parameters and SS_{FF} is the sum of the standard errors of flood frequency. In examining combined effects, SS_{CMBC} is the sum of standard errors of climate models and bias correction methods, SS_{CMFF} the sum of standard errors of climate models and extreme frequency, and SS_{BCHP} is the sum of standard errors of bias correction methods and hydrological parameters.

Results

3.1 Evaluation of bias correction techniques

The annual maximum daily precipitation series from 12 GCMs were evaluated against observations for each catchment during the period 1976-2005 (reference period). RR, MAE, PBIAS and RMSE results for each catchment are presented in Figure 3 and Figure S1. Following bias correction, results indicate an improvement of the GCMs in reproducing observed annual maximum precipitation. However, the performance of each bias correction method is not uniform for all catchments and GCMs. MAE values range from 0 to 195, RMSE 0 to 40, PBIAS -65 to 40, and RR ranges from -0.40 to 0.50. Overall, the distribution based bias correction methods performed better in reproducing observed maximum precipitation in these catchments. The smallest PBIAS is observed in the Boyne catchment and largest in the Newport catchment. The BC-CCSM and ACCES CM2 climate models show high RR (0.4) in the Slaney catchment using DGQM, SGQM and BSM. Whereas GFDL and MPIESM-LR climate models indicates lower performance in correcting precipitation using all bias correction methods. Figure 4 shows the raw GCM outputs together with the results of the five bias correction methods applied to the CMIP6 ensemble in simulating the maximum daily precipitation in each month for each catchment. The corrected precipitation gives a wider spread in winter months (except DGQM and EQM techniques), relative to summer months. However, the ensemble spread is dependent on the bias correction method. DGQM and EQM methods result in a relatively narrower spread, whereas SGQM, BSM and CF return a wide range of simulations (Figure 4).

The influence of each bias correction method on the magnitude of simulated changes in annual maximum daily precipitation for the 2050s (2040-2069) and 2080s (2070-2099) (relative to reference period: 1976-2005) was evaluated for each GCM SSP combination (Figure 5). Simulated changes from the same 12 GCMs using different bias correction approaches show substantial differences in the magnitude of changes in annual maximum precipitation. Generally, projected changes are smaller in the Slaney and Boyne using DG methods, whereas the changes in the Blackwater and Newport are smaller using EQ and SG. There is also a linear relationship between the annual maximum precipitation changes suggested for the 2050s and 2080s,

335 for most bias correction techniques and catchments, indicating a positive trend in the magnitude of changes with time (Figure 5). However, we note that there is greater scatter for EQM relative to other bias correction techniques and in the Blackwater catchment relative to other catchments. We also note that the magnitude of change in annual maximum daily precipitation tends to be higher for SSP585 than for SSP370 and SSP126 and slightly higher in the Slaney and Newport catchments, relative to the Boyne and Blackwater. Changes in annual maximum daily precipitation for SSP126 are smaller than those simulated 340 for SSP370 and SSP585 due to the lower radiative forcing and socio-economic impact associated with SSP126 relative to other scenarios.

3.2 Hydrological modelling and parameter uncertainty evaluation

The GLUE procedure was used to identify a set of model parameters that offer acceptable performance. Thirty thousand parameter sets were randomly generated from uniform distributions with the NSE objective function threshold of > 0.5 345 calculated from daily mean flows used to identify behavioural parameter sets. To produce future simulations, we employ the top 300 behavioural parameter sets. Figure S3 shows the variation in model parameter values and NSE for each GR4J model parameter and catchment. The majority of parameters show clearly identified peaks for each catchment, particularly the parameters X2, X3 and X4. The only parameter to show a lack of identifiability is the X1 parameter (the production storage capacity) in particular in the Newport catchment. This is the smallest of the four catchments and displays large variability in 350 topography, landcover (forestry) and has a lake present in the catchment. Figure 6 shows the ability of the GR4J model to simulate the maximum daily flows in each month using behavioural sets relative to observations for the years 1976-2005, together with the 95 percent confidence intervals of the simulations. Simulations successfully capture the observations, which mostly fall within the 95 percent confidence interval, except in the Boyne catchment, where a portion of the observed maximum flow time series fall outside of the simulated confidence interval. We note that the Boyne catchment has undergone significant 355 arterial drainage works, which is likely to result in higher peak flows (Harrigan et al., 2014) in the observations relative to the model simulated values. GR4J achieved the best fit in the 95% CI modelling discharge in the Newport catchment. Overall, the model was able to capture winter flows well in all catchments, particularly winter peak flow simulations. The biggest discrepancies were observed in modelled flows during late summer, with poorer performance likely associated with use of the NSE objective function which is more sensitive to the large peak values than lower flows in summer.

360

We examined the uncertainty associated with model parameters for different GCMs and future time periods. Figure 7 shows the simulated annual maximum daily flow for the reference and each future time period using the 300 GR4J behavioural parameter sets forced with 12 GCMs bias corrected using DGQM. It is evident that the uncertainty associated with hydrological model parameters is not static and varies depending on climate model, catchment and future time period. The importance of 365 hydrological model uncertainty tends to be greatest for climate models that project the largest magnitude of change indicating that the changing characteristics of precipitation (e.g. mean and variability) have a large bearing on the importance of hydrological model uncertainty. It is also likely that different bias correction techniques interact with parameter uncertainty.

The uncertainties associated with hydrological model parameters tend to be greatest for the 2080s (black lines in Figure 7), and for the Boyne and Slaney catchments.

370

Percent changes in maximum annual daily flow simulated using behavioural parameter sets, 12 ~~G~~CMs bias corrected by each of the five methods, together with the raw simulations are presented in Figure 8. A clear increase in the annual maximum flow is suggested using DGQM, SGQM, CF, EQM and BSM, however, the magnitude of simulated increases differs depending on bias correction approach and are not uniform across the selected catchments. Overall, distribution based bias correction models

375 give smaller changes in annual maximum flow time series. This indicates that wet-day frequency correction is very important for understanding future annual maximum flow projections. Annual maximum flow changes using EQM gives a higher spread range and uncertainty in each catchment, while the change factor method produces the most modest changes. Changes in annual maximum flow are smallest in the Blackwater, which is notable as the catchment with largest groundwater storage. Changes in annual maximum flow are more constrained under SSP126 than SSP370 and SSP585, however differences between

380 SSPs are modest and uncertainty ranges of changes in annual maximum flow are considerable for each (Figure 8).

3.3 Flood quantile projections under varying climate conditions

Figure 9 shows the estimated flood quantile values at different return periods (from 2 year to 100 year) using GEV, LN and LogL distribution models, and associated 95% confidence intervals from 12 ~~G~~CMs (under SSP370 scenario) bias corrected using the DGQM method over the full simulation period (1976-2100). Overall, the LogN distribution returned the smallest

385 flood quantile magnitude, while the estimated quantile values using LogL tend to be largest across each catchment~~, while~~ and hav~~ev~~ing the narrowest uncertainty band~~s using LogL.~~. ~~Overall, the LogN distribution returned the smallest in flood quantile magnitude and the narrowest uncertainty band, while the estimated quantile values using LogL tend to be the largest across each catchment.~~ The GEV distribution ~~gives~~ produces the largest uncertainty ranges in flood quantiles in all catchments (Figure 9).

390

Percent changes in flood quantiles for return periods ranging from 10 to 50 years were also evaluated for each future period under SSP370 using ensemble mean of three distribution types fitted to the median GR4J simulation combining all ~~G~~CMs and bias correction methods (Figure 10); and ~~Figure flood~~ Figure S4 shows the quantile values using the GEV distribution fitted to the median GR4J simulation combining all ~~G~~CMs and DGQM bias correction method~~s~~ (Figure S4). Each catchment shows

395 a significant increase in the magnitude of flood quantiles in the future. Overall, changes in flood quantiles are consistent with changes in annual maxima daily flow and changes depending on the climate period (2020s~~Clim1~~, 2050s~~Clim2~~ and 2080s~~Clim3~~). However, future flood changes are not the same across catchments and differences exist based on bias correction methods employed. The largest changes in flood quantiles across all catchments are found using the BSM bias correction method, where in the Blackwater catchment increases of over 90 percent are found for the 50-year return period in the 2050s

400 and 2080s. Other bias correction techniques return more modest increases. Changes in flood quantiles estimated using the CF

and DGQM approaches show larger changes in the 2050s relative to the 2080s in the Blackwater. Indeed, the CF method shows the most modest changes in all quantiles for the 2080s relative to other time periods across all catchments. In the Slaney most bias correction methods show only small changes in flood quantiles between time periods, the exception being EQM which shows substantial increases in each flood quantile moving across each time-period. The EQM method tends to show the greatest increases in magnitude for higher quantile floods, with largest percent changes returned for the 50-year return period. In the Newport and Boyne catchments, the CF approach shows modest reductions in the magnitude of higher frequency floods, a characteristic not reported using other bias correction techniques. Interestingly, the changes depending on the future climate period with. in most of the catchments showing that higher change in the 2020s than the 2050s. This is likely due to climate variability and nonlinearity climate response; and the climate models suffer to accurately reproducing the whole climate system (natural and anthropogenic)..

3.4 Uncertainty estimation and decomposition for flood quantile estimation

The magnitude of each of the four sources of uncertainty on flood hazard estimation was estimated first based on the additive chain principle to reveal their contribution to the overall uncertainty in projected changes. Projections from each of 12 climate models were iteratively passed through five bias correction techniques and used to force the GR4J model using behavioural parameters sets, before fitting each of the three frequency distributions to estimate future flood hazard. Therefore, for the sensitivity spread forsensitivity climateto climate model uncertaintys was evaluated by varying simulations using each of the 12 GCMs while using atogether with a single bias correction technique, median hydrological model parameter set and a single flood frequency distribution. Figure 11 presents the integrative range of this cascade of uncertainty in estimating return period floods for each catchment using data spanning the years 1976-2100. The dominant source of uncertainty differs from catchment to catchment. Climate models, flood frequency distribution and bias correction techniques tend to be the dominant contributing source of uncertainty in estimating flood quantiles. Using this the one- at- a- time approach to evaluating uncertainties in flood quantiles, climate model projections in the Newport and Blackwater catchments climate model projections present the dominant source of uncertainty, particularly for higher flood quantiles. Notably the relative magnitude of uncertainty in the smaller flood quantiles in the Blackwater catchment is different than for larger flood quantiles, with the extreme value distribution becoming dominant at lower flood quantiles. The largest source of uncertainty in the Slaney is derived from the use of different frequency distribution models. For the Boyne catchment the bias correction methods contribute more to the total uncertainty. Therefore, the various steps in the modelling chain contribute differently in each catchment to total uncertainty in future flood hazard estimation and in some catchments vary depending on the flood quantile of interest (Figure 11).

While additive chains may be useful for evaluating individual components of uncertainty, they do not allow identification of the interactive components of the uncertainty cascade. We use ANOVA to decompose the contribution of individual sources of uncertainty and their interaction in contributing to the total uncertainty in future flood hazard (Figure 12). We evaluate

changes in 10-year, 50-year and 100-year return period flood for the 2080s (2070-2099) relative to the reference period (1976-

435   2005). The decomposition of uncertainty is based on the variance in changes of flood quantile values and calculated out of 100 percent, i.e. the sum of all sources is equal to 100. The contribution of each source of uncertainty is not uniform across the selected catchments (Figure 12). Taking the example of the magnitude of the 100-year flood (Figure 12 outer band), future flood hazard in the Blackwater catchment for the 2080s is highly sensitive to the climate model used (36.5% of total uncertainty in 100-year flood) and respective bias correction methods (20% of total uncertainty). By contrast, future flood frequency in

440   the Boyne is more sensitive to bias correction methods (30.0%) and extreme value distribution (25.5%) employed. In the Boyne catchment, the climate model ensemble accounts for less than one quarter (22.5%) of the uncertainty in simulations of the 100-year flood by the 2080s and is comparable in magnitude to the interactive components of the cascade. In the Newport catchment the use of different extreme value distributions (36.3%) presents the largest component of uncertainty, followed by the climate model ensemble. The results of ANOVA analysis also confirm that the uncertainty resultant from the interaction

445   of the key sources considered is not negligible and also varies on a catchment basis. In the Slaney and Blackwater catchments the interaction of various uncertainty components accounts for 16.8% and 16% of the total uncertainty in estimates of the 100-year flood by the 2080s. By contrast, interactive components in the Newport and Boyne catchments account for approximately one quarter of the uncertainty range (25.2% in the Newport and 22% in the Boyne). Overall, hydrological parameter uncertainty is the least dominant source of uncertainty in future flood frequency estimates across each catchment (Figure 11 and Figure

450   12). For estimates of the 100-year flood in the 2080s (Figure 12 outer band), hydrological model parameter uncertainty is typically 5% of the total uncertainty, reaching up to 9% in the Boyne. Furthermore, the contribution of each of the main components of uncertainty and their interactions to total uncertainty is broadly similar for the different return periods considered for our analysis of the 2080s (Figure 12).

455   **4. Discussion**

We examined future changes in flooding for four catchments in Ireland, including within our modelling chain the uncertainties derived from 12 CMIP6 ~~G~~CMs, ~~5~~ five commonly used bias correction techniques, hydrological model parameters and three flood frequency distributions. We found that maximum precipitation in all catchments is projected to increase over the coming

460   decades, however changes are not uniform across catchments. The largest change in annual maximum precipitation was found for the Newport catchment, with ensemble median increases becoming progressively larger for the 2020s, 2050s and 2080s (27%, 40%, 60%, respectively). In the Slaney catchment, increases in annual maximum precipitation between the 2050s and 2080s are not statistically significant. In the Blackwater catchment, most of the climate models indicate a positive change but these have a wide range of uncertainty relative to other catchments (from 0 to 55% in 2050s and 0 to 60% in 2080s). We find

465   projected changes in flood magnitudes to be broadly proportional to changes in maximum precipitation in all catchments. Projected changes in flood magnitude are higher using the SSP585 and lower using SSP126 climate scenarios. Overall changes

in precipitation and air temperature are broadly consistent with previous findings using CMIP5 (Broderick et al., 2019) in Ireland.

470 Our findings demonstrate the large uncertainties associated with projected flood magnitudes ~~with climate change~~. Over recent years much research has sought to explore the dominant sources of uncertainty in climate change impact assessments. Similar studies have identified climate models as being the dominant source (e.g. Sulis et al., 2012; Hattermann et al., 2018). Indeed ~~(~~Addor et al.~~,~~ ~~((~~2014) highlight that there seems to be a general agreement in the literature on the dominant contribution of climate models to the uncertainty in discharge projections. ~~On the contrary~~In contrast, our findings demonstrate the challenges

475 of generalising about the dominant components of the cascade of uncertainty at the catchment scale, important for understanding future flood risk. Using both additive chains and variance decomposition to examine components of the modelling chain employed, our results show that not only does the contribution and importance of different components of the modelling chain vary across catchments, but that the dominant source of uncertainty can be completely different. Moreover, the dominant sources of uncertainty vary depending on which approach is used to evaluate uncertainty. Using additive chains,

480 in two of our study catchments, the climate model ensemble was the dominant source of uncertainty, as was expected. However, for the ~~other two catchments, namely the~~ Boyne and the Slaney, the extreme value distribution employed for flood frequency analysis and the bias correction method used to adjust raw GCM output contribute greater uncertainty to future flood risk than the ensemble of ~~G~~CMs employed. Using variance decomposition ~~that~~ allows for the interaction of components of the modelling chain to be evaluated and quantified and offers a fuller assessment of uncertainty. Our result show that in the Slaney

485 and Blackwater catchments the climate model ensemble used dominated the cascade of uncertainty. In the Slaney, the second most important component is the bias correction technique used, while in the Blackwater the frequency distribution model ~~comes~~ is the second most important component. In the Newport catchment, the flood frequency distribution model ~~used~~ ranks as the most important component of the cascade of uncertainty, followed by the climate model ensemble. Finally, in the Boyne catchment, the climate model ensemble ranks as only the third most important component of the uncertainty cascade in

490 simulating flood quantiles, with the bias correction methods coming first and the flood frequency distribution second.

We hypothesise ~~how~~ that catchment characteristics may influence the dominant components of the cascade of uncertainty in each catchment. The Slaney and Blackwater, where climate models dominate, are among the largest in our sample with groundwater contributing significantly to runoff in both. In the Blackwater catchment topography has a large bearing on flood

495 response time within the catchment with flood peaks moving more rapidly from elevated sub-catchments into the main channel and may be a reason as to why the flood frequency model ranks as the second dominant component in the cascade of uncertainty. The Slaney catchment drains the southern component of the Wicklow mountains before reaching shallower elevations as it flows south through Carlow and Wexford. The variation in topography and hence precipitation from upper to lower reaches may be a reason as to why bias correction methods emerge as the second most important component of the

500 uncertainty cascade in this catchment. The Newport catchment is the smallest in our sample with flood response influenced

more strongly by varied land use cover (forestry, rotational cropping) and the presence of a lake in the upper reaches of the catchment. The flood frequency distribution dominates the cascade, followed by the climate model ensemble used. Finally, the Boyne catchment has been heavily influenced by arterial drainage works, resulting in the insertion of field drains and the deepening and widening of the river channel (Harrigan et al., 2014). These interventions have resulted in a faster rainfall runoff response. In the Boyne catchment therefore, projected changes in future rainfall are likely to have a more direct bearing on the flood response, with uncertainty in bias correction and the flood frequency distribution dominating the cascade of uncertainty.

Across each of our catchments and in the context of the modelling chain employed, the uncertainty from hydrological model parameters is the smallest component of total uncertainty in the estimation of future flood hazard magnitude. Bastola et al. (2011a; 2011 b) identify hydrological model uncertainty as important in a previous assessment of change in flood risk, while Mizukami et al. (2016) rank hydrological model uncertainty of greater importance than bias correction approaches in US catchments. We note that we do not consider hydrological model structure uncertainty in our modelling chain and that our decision to select only the top 300 behavioural parameter sets, rather than all those identified may be a factor here. This highlights how subjective decisions in the application of hydrological models may have important implications for the uncertainty in future projections (Melsen et al., 2019). We also find that the contribution to total uncertainty from the interaction of components within the modelling chain is substantial – up to one quarter of the uncertainty range considered in two catchments.

While uncertainty decomposition may be useful in helping scientists navigate the cascade of uncertainty by prioritising the key components of the uncertainty cascade to sample (Clark et al., 2016) for a particular catchment, our small sample makes it difficult to determine how catchment characteristics may be informative in identifying the dominant sources of uncertainty a priori. There are some indications that catchment properties and the characteristics of observed precipitation may influence which uncertainties may dominate. Vetter et al. (2017) used variance decomposition to examine the contribution of modelling chains (GCM, emissions scenario (in the form of Representative Concentration Pathways (RCPs)) and hydrological model) to total uncertainty in different parts of the flow regime. In their study, they examine 12 large catchments globally. While Vetter et al. (2017) highlight the dominance of GCMs in total uncertainty across many catchments they highlight that the share of emissions scenario and hydrological model contributions to overall uncertainty can differ between catchments. Similar to our findings, Vetter et al. (2017) highlight the importance of interacting components of the modelling chain employed.

As our study has shown, the evaluation of uncertainties and their interaction in future flood risk assessment with climate change is a critical step in understanding future impacts and informing adaptation decision making. However, results depend on the modelling chain employed and the method used to quantify uncertainties. Given the possibility of examining interactive components of modelling chain, we recommend the use of ANOVA based techniques to decompose the cascade of uncertainty. We highlight however that our modelling chain is not complete and that the work presented here is illustrative rather than

535 exhaustive. We do not, for example, include uncertainties in future flood estimates derived from different hydrological model structures with previous work, as indicated above, showing that hydrological model structure and complexity may be an important component of future uncertainties. Other potential sources of hydrological model uncertainty are also omitted. For example, we did not evaluate the transferability of parameter sets to represent future rainfall runoff response (e.g. Broderick et al. 2016), nor did we evaluate the influence that selection of different objective functions may have on the identification of

540 behavioural parameter sets. Westerberg et al. (2020) also highlight the potential importance of uncertainty in the discharge data used to calibrate hydrological models. In assessing different flood quantiles, we use only 30 years of annual maxima to extrapolate to return periods outside our record length. Such extrapolations should be treated cautiously but are prevalent in many studies (e.g. Alison L. Kay et al., 2006; Lawrence, 2020; Meresa and Romanowicz, 2017) while rarer floods are also associated with design standards (e.g. 100-year flood) and therefore of interest to decision makers. We also assume that flood

545 processes remain stationary within the 30-year windows used to evaluate changes, while other factors that can influence rainfall runoff response, such as land use change, remain unchanged from the calibration period used to train our hydrological models.

5. Conclusions

This study evaluates changes in future flood magnitude with climate change for four Irish catchments using a modelling chain

550 incorporating 12 ~~G~~CMs comprising the CMIP6 ensemble, 5 bias correction techniques, hydrological model parameter uncertainty and the use of extreme value distributions. Our findings suggest increasing flood hazards over the coming decades in all catchments, with changes in flooding largely consistent with changes in maximum precipitation. However, uncertainties in future flood changes are large and increase with time and flood quantile. Using ANOVA, we decompose uncertainties in future flood quantiles to examine how individual components of our modelling chain and their interactions contribute to overall

555 uncertainty. Our results show how the dominant sources of uncertainty may vary on a catchment basis, highlighting the inability to generalise on the dominant components of uncertainty across catchments. Across all four catchments the climate models, bias correction methods and the extreme value distributions used to evaluate flood return periods were differentially dominant, while the uncertainty derived from the interaction of various components was substantial in all catchments. Our work shows the value of ANOVA methods in visualising and quantifying the uncertainty cascade at a catchment level which

560 will be helpful in navigating the uncertainties associated with future flood risk for better adaptation decision making. While our sample is small, the dominant components of uncertainty in future flood risk may be related to catchment characteristics. We therefore recommend that future work seeks to better understand the link between the key components of the cascade of uncertainty and catchment characteristics. Ability to do so would offer considerable advantages in knowing a-priori which sources of uncertainty should be targeted as priority.

565

Acknowledgements

We thank data providers and three reviewers for their constructive comments and feedback which helped improve our manuscript.

Funding

This work was made possible by the award of funding from the Office of Public Works and Kildare County Council to HM, CM and RF.

Author contributions

HM designed the study with input from CM, RF. HM conceived the model and the computational framework and analysed. HM wrote the manuscript with input from all authors.

Conflict of interest

The authors declare no competing interests. None

References

Addor, N., O. Rossler, N. K € oplin, M. €, Huss, R. Weingartner, and J. S., & (2014). (2014). Water Resources Research. *Robust Changes and Sources of Projected, Uncertainty in the Swiss, Hydrological Regimes of Catchments, Water Resour. Res., 50 7541–7562, Doi:10.1002/ 2014WR015549*, 5375–5377. https://doi.org/10.1002/2013WR014979.Reply

Bastola, S., Murphy, C., & Sweeney, J. (2011a). The role of hydrological modelling uncertainties in climate change impact assessments of Irish river catchments. *Advances in Water Resources*, *34*(5), 562–576. https://doi.org/10.1016/j.advwatres.2011.01.008

Bastola, S., Murphy, C., & Sweeney, J. (2011b). The sensitivity of fluvial flood risk in Irish catchments to the range of IPCC AR4 climate change scenarios. *Science of the Total Environment*, *409*(24), 5403–5415. https://doi.org/10.1016/j.scitotenv.2011.08.042

Beven, K., & Binley, A. (1992). The future of distributed models: Model calibration and uncertainty prediction. *Hydrological Processes*, *6*(3), 279–298. https://doi.org/10.1002/hyp.3360060305

Blöschl, G., Bierkens, M. F. P., Chambel, A., Cudennec, C., Destouni, G., Fiori, A., Kirchner, J. W., McDonnell, J. J., Savenije, H. H. G., Sivapalan, M., Stumpp, C., Toth, E., Volpi, E., Carr, G., Lupton, C., Salinas, J., Széles, B., Viglione, A., Aksoy, H., … Zhang, Y. (2019). Twenty-three unsolved problems in hydrology (UPH)–a community perspective. *Hydrological*

Sciences Journal, *64*(10), 1141–1158. https://doi.org/10.1080/02626667.2019.1620507

600   Blöschl, G., Hall, J., Parajka, J., Perdigão, R. A. P., Merz, B., Arheimer, B., Aronica, G. T., Bilibashi, A., Bonacci, O., Borga, M., Čanjevac, I., Castellarin, A., Chirico, G. B., Claps, P., Fiala, K., Frolova, N., Gorbachova, L., Gül, A., Hannaford, J., … Živković, N. (2017). Changing climate shifts timing of European floods. *Science*, *357*(6351), 588–590. https://doi.org/10.1126/science.aan2506

Bosshard, T., M. Carambia, K. Goergen, S. Kotlarski, P. Krahe, M. Zappa, and C. Schär (2013), Quantifying uncertainty
605   sources in an ensemble of hydrological climate-impact projections, *Water Resour. Res.*, 49, 1523–1536, doi:10.1029/2011WR011533

Broderick, C., Murphy, C., Wilby, R. L., Matthews, T., Prudhomme, C., & Adamson, M. (2019). Using a Scenario-Neutral Framework to Avoid Potential Maladaptation to Future Flood Risk. *Water Resources Research*. https://doi.org/10.1029/2018WR023623

610   Broderick, C., T. Matthews, R. L. Wilby, S. Bastola, and C. Murphy (2016), Transferability of hydrological models and ensemble averaging methods between contrasting climatic periods, Water Resour. Res., 52, 8343–8373, doi:10.1002/2016WR018850

Chen, J., Brissette, F. P., Chaumont, D., & Braun, M. (2013). Finding appropriate bias correction methods in downscaling precipitation for hydrologic impact studies over North America. *Water Resources Research*, *49*(7), 4187–4205.
615   https://doi.org/10.1002/wrcr.20331

Chen, L., Singh, V. P., Shenglian, G., Hao, Z., & Li, T. (2012). Flood Coincidence Risk Analysis Using Multivariate Copula Functions. *Journal of Hydrologic Engineering*, *17*(6), 742–755. https://doi.org/10.1061/(ASCE)HE.1943-5584.0000504

Ciaran Broderick, Tom Matthews, Robert L. Wilby, Satish Bastola, and C. M. (1969). Water Resources Research. *Journal of the American Water Resources Association*, *5*(3), 2–2. https://doi.org/10.1111/j.1752-1688.1969.tb04897.x

620   Clark, M. P., Wilby, R. L., Gutmann, E. D., Vano, J. A., Gangopadhyay, S., Wood, A. W., Fowler, H. J., Prudhomme, C., Arnold, J. R., & Brekke, L. D. (2016). Characterizing Uncertainty of the Hydrologic Impacts of Climate Change. *Current Climate Change Reports*, *2*(2), 55–64. https://doi.org/10.1007/s40641-016-0034-x

Dobler, C., Hagemann, S., Wilby, R. L., & StÃtter, J. (2012). Quantifying different sources of uncertainty in hydrological projections in an Alpine watershed. *Hydrology and Earth System Sciences*, *16*(11), 4343–4360.
625   https://doi.org/10.5194/hess-16-4343-2012

Ehret, U., Zehe, E., Wulfmeyer, V., Warrach-Sagi, K., & Liebert, J. (2012). HESS Opinions "should we apply bias correction to global and regional climate model data?" *Hydrology and Earth System Sciences*, *16*(9), 3391–3404. https://doi.org/10.5194/hess-16-3391-2012

Fowler, H. J., Ekström, M., Blenkinsop, S., & Smith, A. P. (2007). Estimating change in extreme European precipitation using
630   a multimodel ensemble. *Journal of Geophysical Research Atmospheres*, *112*(18). https://doi.org/10.1029/2007JD008619

GIORGI, F., & GAO, X. J. (2018). Regional earth system modeling: review and future directions. *Atmospheric and Oceanic Science Letters*, *11*(2), 189–197. https://doi.org/10.1080/16742834.2018.1452520

Giuntoli, I., Villarini, G., Prudhomme, C., & Hannah, D. M. (2018). Uncertainties in projected runoff over the conterminous United States. *Climatic Change*, *150*(3–4), 149–162. https://doi.org/10.1007/s10584-018-2280-5

635 Gosling, S. N., Taylor, R. G., Arnell, N. W., & Todd, M. C. (2011). A comparative analysis of projected impacts of climate change on river runoff from global and catchment-scale hydrological models. *Hydrology and Earth System Sciences*, *15*(1), 279–294. https://doi.org/10.5194/hess-15-279-2011

Griffis, V. W., & Stedinger, J. R. (2007). *Evolution of Flood Frequency Analysis with Bulletin 17*. June, 283–297.

Gudmundsson, L., Wagener, T., Tallaksen, L. M., & Engeland, K. (2012). Evaluation of nine large-scale hydrological models
640 with respect to the seasonal runoff climatology in Europe. *Water Resources Research*, *48*(11). https://doi.org/10.1029/2011WR010911

Gutjahr, O., & Heinemann, G. (2013). Comparing precipitation bias correction methods for high-resolution regional climate simulations using COSMO-CLM: Effects on extreme values and climate change signal. *Theoretical and Applied Climatology*, *114*(3–4), 511–529. https://doi.org/10.1007/s00704-013-0834-z

645 Hamon, W. R. (1964). Computation of direct runoff amounts from storm rainfall. In *General Assembly of Berkeley, Symposium on Surface Waters: Vol. Extract of* (pp. 52–62).

Harrigan, S., Murphy, C., Hall, J., Wilby, R. L., & Sweeney, J. (2014). Attribution of detected changes in streamflow using multiple working hypotheses. *Hydrology and Earth System Sciences*, *18*(5), 1935–1952. https://doi.org/10.5194/hess-18-1935-2014

650 Hattermann, F. F., Vetter, T., Breuer, L., Su, B., Daggupati, P., Donnelly, C., Fekete, B., Florke, F., Gosling, S. N., Hoffmann, P., Liersch, S., Masaki, Y., Motovilov, Y., Muller, C., Samaniego, L., Stacke, T., Wada, Y., Yang, T., & Krysnaova, V. (2018). Sources of uncertainty in hydrological climate impact assessment: A cross-scale study. *Environmental Research Letters*, *13*(1). https://doi.org/10.1088/1748-9326/aa9938

He, S., Guo, S., Liu, Z., Yin, J., Chen, K., & Wu, X. (2018). Uncertainty analysis of hydrological multi-model ensembles
655 based on CBP-BMA method. *Hydrology Research*, *49*(5), 1636–1651. https://doi.org/10.2166/nh.2018.160

Hughes, D. A., Kingston, D. G., & Todd, M. C. (2011). Uncertainty in water resources availability in the Okavango River basin as a result of climate change. *Hydrology and Earth System Sciences*, *15*(3), 931–941. https://doi.org/10.5194/hess-15-931-2011

IPCC. (2013). IPCC CLIMATE CHANGE 2013 Climate Change 2013. In *Researchgate.Net*.
660 https://doi.org/10.1017/CBO9781107415324.Summary

Jobst, A. M., Kingston, D. G., Cullen, N. J., & Schmid, J. (2018). Intercomparison of different uncertainty sources in hydrological climate change projections for an alpine catchment (upper Clutha River, New Zealand). *Hydrology and Earth System Sciences*, *22*(6), 3125–3142. https://doi.org/10.5194/hess-22-3125-2018

Kay, A. L., Davies, H. N., Bell, V. A., & Jones, R. G. (2009). Comparison of uncertainty sources for climate change impacts:
665 Flood frequency in England. *Climatic Change*, *92*(1–2), 41–63. https://doi.org/10.1007/s10584-008-9471-4

Kay, Alison L., Jones, R. G., & Reynard, N. S. (2006). RCM rainfall for UK flood frequency estimation. II. Climate change

results. *Journal of Hydrology*, *318*(1–4), 163–172. https://doi.org/10.1016/j.jhydrol.2005.06.013

Knutti, R., & Sedláček, J. (2013). Robustness and uncertainties in the new CMIP5 climate model projections. *Nature Climate Change*, *3*(4), 369–373. https://doi.org/10.1038/nclimate1716

670 Krinner, G., & Flanner, M. G. (2018). Striking stationarity of large-scale climate model bias patterns under strong climate change. *Proceedings of the National Academy of Sciences of the United States of America*, *115*(38), 9462–9466. https://doi.org/10.1073/pnas.1807912115

Lafon, T., Dadson, S., Buys, G., & Prudhomme, C. (2013). Bias correction of daily precipitation simulated by a regional climate model: A comparison of methods. *International Journal of Climatology*, *33*(6), 1367–1381.
675 https://doi.org/10.1002/joc.3518

Lawrence, D. (2020). Uncertainty introduced by flood frequency analysis in projections for changes in flood magnitudes under a future climate in Norway. *Journal of Hydrology: Regional Studies*, *28*(December 2019), 100675. https://doi.org/10.1016/j.ejrh.2020.100675

Li, L., Xu, C. Y., Xia, J., Engeland, K., & Reggiani, P. (2011). Uncertainty estimates by Bayesian method with likelihood of
680 AR (1) plus Normal model and AR (1) plus Multi-Normal model in different time-scales hydrological models. *Journal of Hydrology*, *406*(1–2), 54–65. https://doi.org/10.1016/j.jhydrol.2011.05.052

Mazzorana, B., Levaggi, L., Keiler, M., & Fuchs, S. (2012). Towards dynamics in flood risk assessment. *Natural Hazards and Earth System Science*, *12*(11), 3571–3587. https://doi.org/10.5194/nhess-12-3571-2012

Melsen, L. A., Teuling, A. J., Torfs, P. J. J. F., Zappa, M., Mizukami, N., Mendoza, P. A., Clark, M. P., & Uijlenhoet, R.
685 (2019). Subjective modeling decisions can significantly impact the simulation of flood and drought events. *Journal of Hydrology*, *568*(November 2018), 1093–1104. https://doi.org/10.1016/j.jhydrol.2018.11.046

Meresa, H.K., & Romanowicz, R. J. (2017). The critical role of uncertainty in projections of hydrological extremes. *Hydrology and Earth System Sciences*, *21*(8). https://doi.org/10.5194/hess-21-4245-2017

Meresa, Hadush K., & Gatachew, M. T. (2019). Climate change impact on river flow extremes in the upper blue nile river
690 basin. *Journal of Water and Climate Change*, *10*(4), 759–781. https://doi.org/10.2166/wcc.2018.154

Meresa, Hadush K., & Romanowicz, R. J. (2017). The critical role of uncertainty in projections of hydrological extremes. *Hydrology and Earth System Sciences*. https://doi.org/10.5194/hess-21-4245-2017

Meresa, Hadush K, Romanowicz, R. J., & Napiorkowski, J. J. (2017). Understanding changes and trends in projected hydroclimatic indices in selected Norwegian and Polish catchments. *Acta Geophysica*, *65*(4), 829–848.
695 https://doi.org/10.1007/s11600-017-0062-5

Meresa, Hadush Kidane. (2020). River flow characteristics and changes under the influence of varying climate conditions. *Natural Resource Modeling*, *33*(1), 1–30. https://doi.org/10.1111/nrm.12242

Mizukami, N., Clark, M. P., Gutmann, E. D., Mendoza, P. A., Newman, A. J., Nijssen, B., Livneh, B., Hay, L. E., Arnold, J. R., & Brekke, L. D. (2016). Implications of the methodological choices for hydrologic portrayals of climate change over
700 the contiguous united states: Statistically downscaled forcing data and hydrologic models. *Journal of Hydrometeorology*,

17(1), 73–98. https://doi.org/10.1175/JHM-D-14-0187.1

Osuch, M., Lawrence, D., Meresa, H. K., Napiorkowski, J. J., & Romanowicz, R. J. (2017). Projected changes in flood indices in selected catchments in Poland in the 21st century. *Stochastic Environmental Research and Risk Assessment*, *31*(9). https://doi.org/10.1007/s00477-016-1296-5

Osuch, M., Romanowicz, R. J., Lawrence, D., & Wong, W. K. (2015). Assessment of the influence of bias correction on meteorological drought projections for Poland. *Hydrology and Earth System Sciences Discussions*, *12*(10), 10331–10377. https://doi.org/10.5194/hessd-12-10331-2015

Osuch, Marzena, Romanowicz, R. J., Lawrence, D., & Wong, W. K. (2016). Trends in projections of standardized precipitation indices in a future climate in Poland. *Hydrology and Earth System Sciences*, *20*(5), 1947–1969. https://doi.org/10.5194/hess-20-1947-2016

Peleg, N., Shamir, E., Georgakakos, K. P., & Morin, E. (2015). *A framework for assessing hydrological regime sensitivity to climate change in a convective rainfall environment : a case study of two medium-sized eastern Mediterranean catchments , Israel*. *2*, 567–581. https://doi.org/10.5194/hess-19-567-2015

Perrin, C., Michel, C., & Andréassian, V. (2003). Improvement of a parsimonious model for streamflow simulation. *Journal of Hydrology*, *279*(1–4), 275–289. https://doi.org/10.1016/S0022-1694(03)00225-7

Piani, C., Haerter, J. O., & Coppola, E. (2010). Statistical bias correction for daily precipitation in regional climate models over Europe. *Theoretical and Applied Climatology*, *99*(1–2), 187–192. https://doi.org/10.1007/s00704-009-0134-9

Prudhomme, C., Parry, S., Hannaford, J., Clark, D. B., Hagemann, S., & Voss, F. (2011). How well do large-scale models reproduce regional hydrological extremes: In Europe? *Journal of Hydrometeorology*, *12*(6), 1181–1204. https://doi.org/10.1175/2011JHM1387.1

Raff, D. A., & Rasmussen, R. M. (2014). *used for water resource assessments in the United States*. 7167–7186. https://doi.org/10.1002/2014WR015559.Received

Rojas, R., Feyen, L., & Watkiss, P. (2013). Climate change and river floods in the European Union: Socio-economic consequences and the costs and benefits of adaptation. *Global Environmental Change*, *23*(6), 1737–1751. https://doi.org/10.1016/j.gloenvcha.2013.08.006

Saini, R., Wang, G., Yu, M., & Kim, J. (2015). Phytoplankton light absorption and the package effect in relation to photosynthetic and photoprotective pigments in the northern tip of Antarctic Peninsula. *Journal of Geophical Research*, 3679–3699. https://doi.org/10.1002/2014JD022599.Received

Shepherd, T. G., Boyd, E., Calel, R. A., Chapman, S. C., Dessai, S., Dima-west, I. M., Fowler, H. J., & James, R. (2018). *Storylines : an alternative approach to representing uncertainty in physical aspects of climate change*. 555–571.

Smith, K. A., Wilby, R. L., Broderick, C., Prudhomme, C., Matthews, T., Harrigan, S., & Murphy, C. (2018). Navigating Cascades of Uncertainty — As Easy as ABC? Not Quite…. *Journal of Extreme Events*, *05*(01), 1850007. https://doi.org/10.1142/s2345737618500070

Soriano, E., Mediero, L., & Garijo, C. (2019). Selection of bias correction methods to assess the impact of climate change on

735   flood frequency curves. *Water (Switzerland)*, *11*(11). https://doi.org/10.3390/w11112266

Sulis, M., Paniconi, C., Marrocu, M., Huard, D., & Chaumont, D. (2012). Hydrologic response to multimodel climate output using a physically based model of groundwater/surface water interactions. *Water Resources Research*, *48*(12), 1–18. https://doi.org/10.1029/2012WR012304

Teng, J., Vaze, J., Chiew, F. H. S., Wang, B., & Perraud, J. M. (2012). Estimating the relative uncertainties sourced from GCMs and hydrological models in modeling climate change impact on runoff. *Journal of Hydrometeorology*, *13*(1), 122–139. https://doi.org/10.1175/JHM-D-11-058.1

Teutschbein, C., & Seibert, J. (2013). Is bias correction of regional climate model (RCM) simulations possible for non-stationary conditions. *Hydrology and Earth System Sciences*, *17*(12), 5061–5077. https://doi.org/10.5194/hess-17-5061-2013

Vetter, T., Reinhardt, J., Flörke, M., Griensven, A. Van, Hattermann, F., Seidou, O., Su, B., & Vervoort, R. W. (2016). Evaluation of sources of uncertainty in projected hydrological changes under climate change in 12 large-scale river basins. *Climatic Change*. https://doi.org/10.1007/s10584-016-1794-y

Vetter, T., Reinhardt, J., Flörke, M., van Griensven, A., Hattermann, F., Huang, S., Koch, H., Pechlivanidis, I. G., Plötner, S., Seidou, O., Su, B., Vervoort, R. W., & Krysanova, V. (2017). Evaluation of sources of uncertainty in projected hydrological changes under climate change in 12 large-scale river basins. *Climatic Change*, *141*(3), 419–433. https://doi.org/10.1007/s10584-016-1794-y

Walsh, S. (2012). a Summary of Climate Averages. *The Irish Meteorological Service*, *582*(417). www.met.ie

Westerberg, I. K., Sikorska-Senoner, A. E., Viviroli, D., Vis, M., & Seibert, J. (2020). Hydrological model calibration with uncertain discharge data. *Hydrological Sciences Journal*, *0*(0). https://doi.org/10.1080/02626667.2020.1735638

Wilby, R. L., & Harris, I. (2006). A framework for assessing uncertainties in climate change impacts: Low-flow scenarios for the River Thames, UK. *Water Resources Research*, *42*(2), 1–10. https://doi.org/10.1029/2005WR004065

Wilby, R., Murphy, C., Wilby, R., & Murphy, C. (2019). Decision-Making by Water Managers Despite Climate Uncertainty. In *The Oxford Handbook of Planning for Climate Change Hazards* (Issue February). https://doi.org/10.1093/oxfordhb/9780190455811.013.52

Wyser, K., van Noije, T., Yang, S., von Hardenberg, J., O'Donnell, D., & Döscher, R. (2019). On the increased climate sensitivity in the EC-Earth model from CMIP5 to CMIP6. *Geoscientific Model Development Discussions*, *November*, 1–13. https://doi.org/10.5194/gmd-2019-282

Xu, L. L. C. (2014). *The comparison of sensitivity analysis of hydrological uncertainty estimates by GLUE and Bayesian method under the impact of precipitation errors*. 491–504. https://doi.org/10.1007/s00477-013-0767-1

Yang, W., Andréasson, J., Graham, L. P., Olsson, J., Rosberg, J., & Wetterhall, F. (2010). Distribution-based scaling to improve usability of regional climate model projections for hydrological climate change impacts studies. *Hydrology Research*, *41*(3–4), 211–229. https://doi.org/10.2166/nh.2010.004

770

775

780
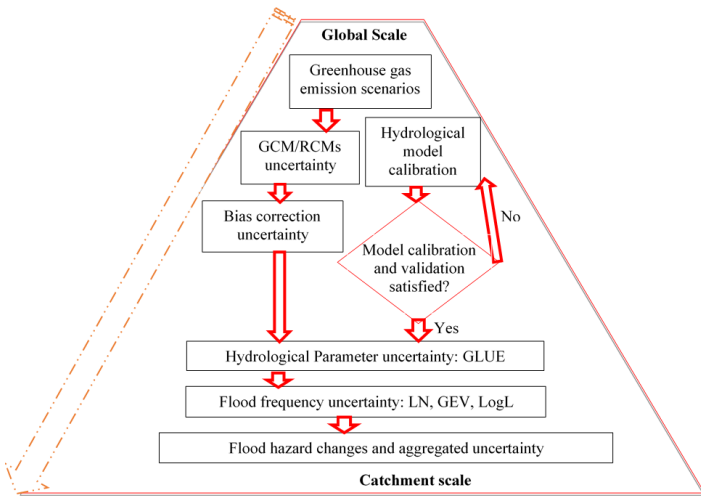
785 **Figure 1.** Research flow chart to estimate projections of flood hazard and identify associated uncertainty
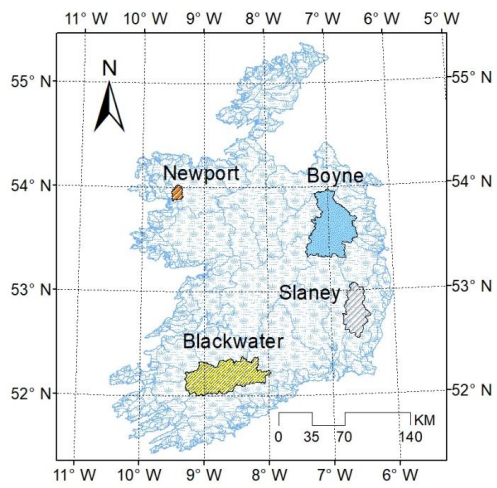
Figure 2. Location of the selected study catchments.

790
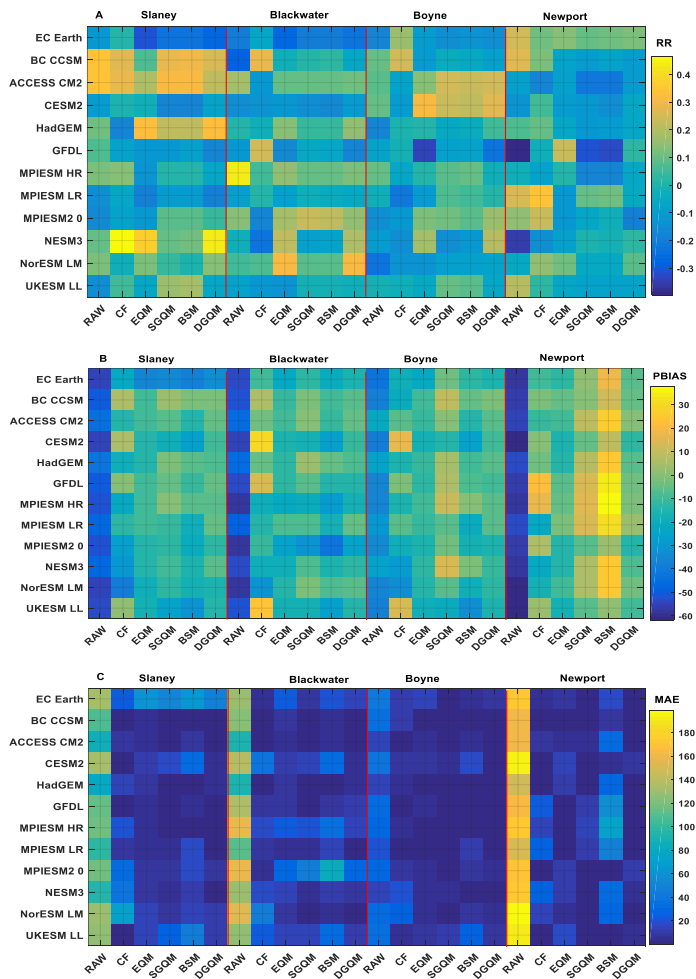
Figure 3 Comparison of corrected annual maximum daily precipitation using five bias correction methods and observed annual maximum precipitation using a) Pearson correlation coefficient (RR), b) Percent Bias (PBIAS) and c) Mean Absolute Error (MAE). The y-axis indicates each of 12 CMIP6 climate models and the x-axis represents each of 5 climate bias correction method.

800
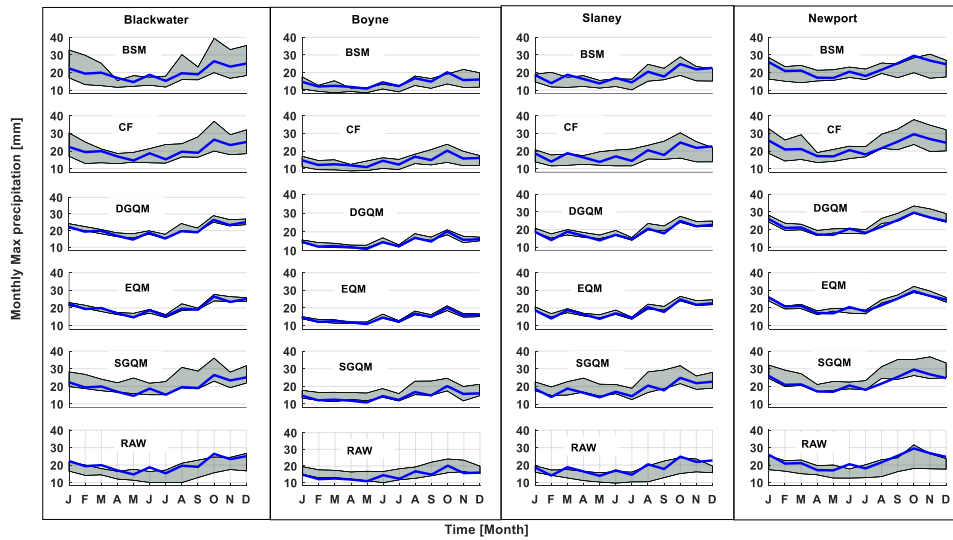
Figure 4 Comparison of raw and bias corrected simulations from 12 CMIP6 GCMs with observed maximum daily precipitation in each month for each of our four study catchments. Each row presents results of one of five bias correction techniques (top row - Birnbaum Distribution (BSM), second row-Change Factors (CF), third row- Double Quantile Mapping
805 using Gamma Distribution (DGQM), fourth row-Empirical Quantile Mapping using Simple Interpolation (EQM), fifth row-Single Quantile Mapping using Gamma Distribution (SGQM), and the last row is the raw GCMs output). In each panel the grey shaded region represents the spread of 12 GCM simulations, with blue line being the observed maximum precipitation.

810
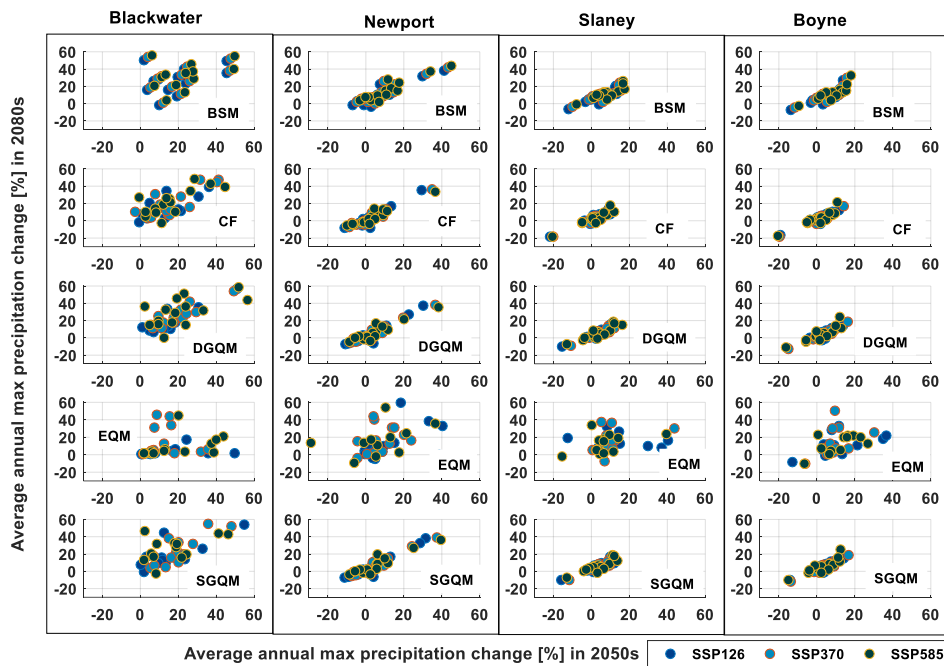
Figure 5. Scatter plots of change in maximum annual daily precipitation as simulated by 12 CMIP6 GCMs (each dot) corrected using each of the five bias correction techniques for three SSP scenarios for the 2050s (2040-2069) and 2080s (2070-2099). 815 The dark blue circle represents SSP126, light blue represents SSP370 and dark green represents SSP585.
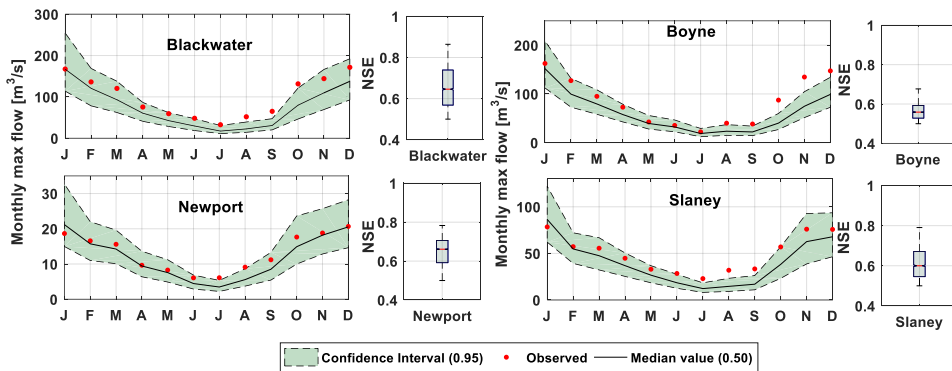
Figure 6. Observed and simulated monthly maximum daily flows (m³/s) using GR4J behavioural parameter sets for the reference period (1976-2005). The black line and shaded area represent the median and 95 percent confidence interval of simulated flows, respectively, the red dot represents observations. Boxplots show the spread in NSE scores for behavioural parameters sets in each catchment.
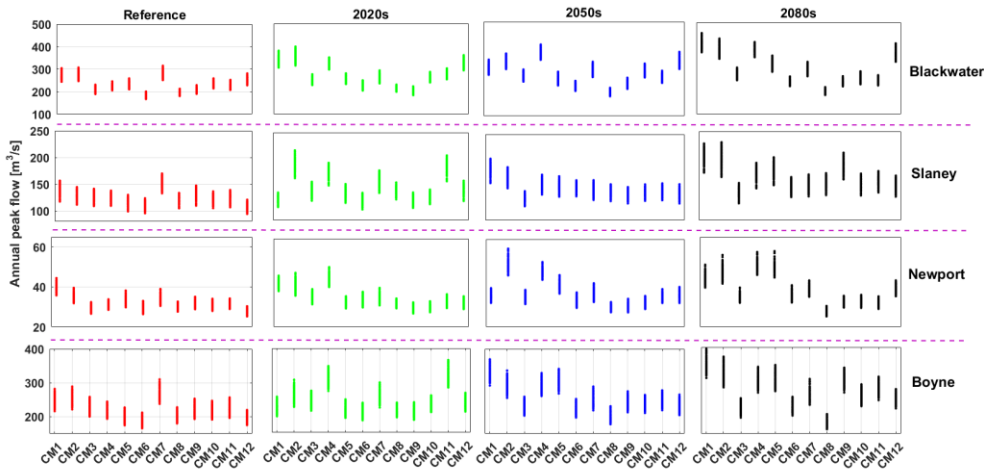
Figure 7. Hydrological model parameter uncertainty in simulating the annual maximum daily flow in each catchment using the best 300 parameter sets for each climate model for the reference period (red), the 2020s (green), 2050s (blue) and 2080s (black) under SSP370 scenario and DGQM bias correction method.
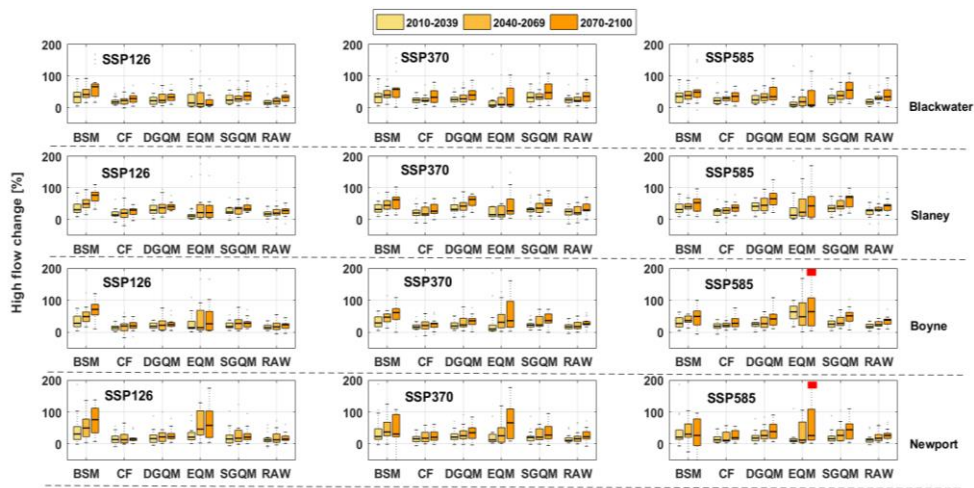
830 **Figure 8.** Matrix of projected percent changes in annual maximum daily flow for the 2020s (2010-2039), 2050s (2040-2069), and 2080s (2070-2099) for SSP126, SSP370 and SSP585 in each catchment with respect to the reference period (1976-2005). Each box plot represents the spread of 12 GCMs for each of the five bias correction techniques as simulated using behavioural model parameter sets. Marked for each boxplot are the median and 0.25 and 0.75 quantiles. The red dots are outliers (changes above 200%).
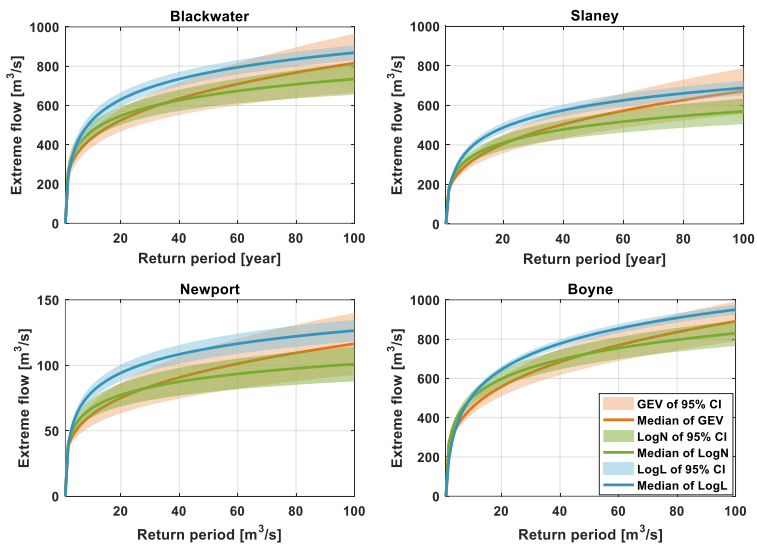
835

Figure 9. Comparison of flood quantiles estimated using three flood distribution models (LogL, GEV and LN) fitted to projected annual maxima series derived from 12 GCMs bias corrected using the DGQM method. The shaded region indicates the 95% confidence interval of annual maximum projections from 12 GCMs under SSP370 scenario over the full projection period (1970-2100 period) in each catchment.

840
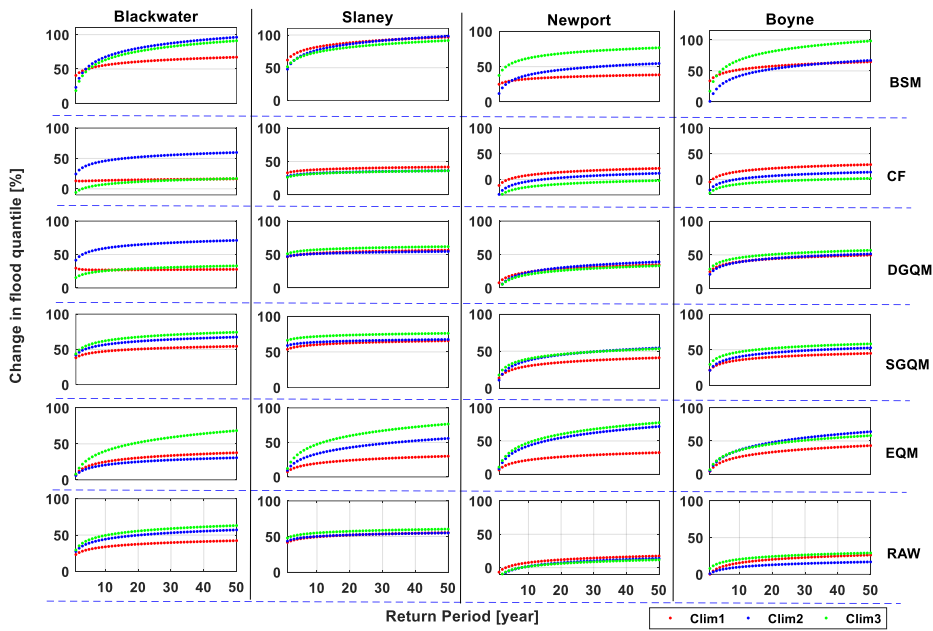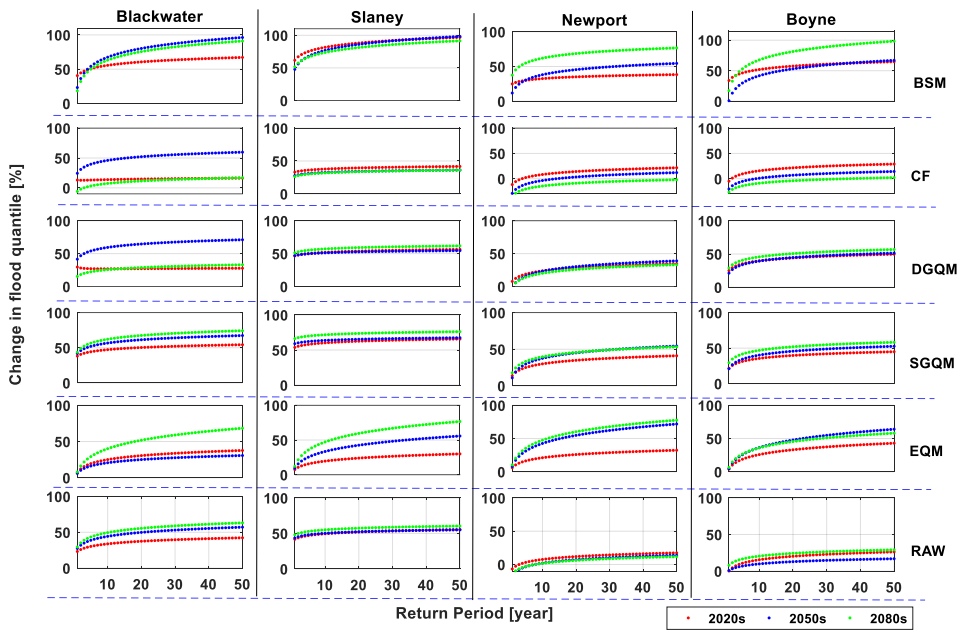
845 **Figure 10**. Percent changes in extreme flow quantiles using ensemble mean of three distribution types, 12 GCMs and 300 parameter sets in each catchment for the 2020s (red), 2050s (blue) and 2080s (green). Simulated changes are derived using raw (bottom row) and bias corrected (the first four rows) simulations.

850

855

860
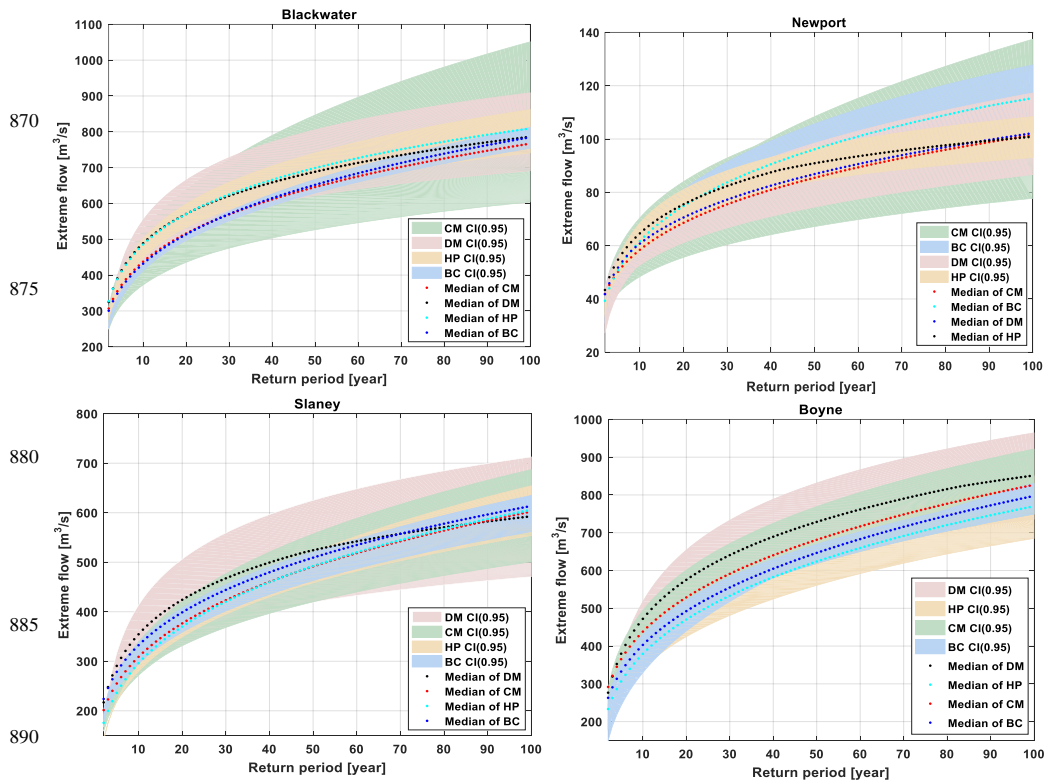
Figure 11. Total uncertainty in flood frequency curve using 12 CMIP6 GCMs (CM), 5 bias correction methods (BC), 300 behavioural parameter sets (HP) and 3 extreme value distributions (DM). Shaded areas represent the 95 percent confidence interval for each component in the modelling chain while the dotted line stands for their respective median values. The curves are fitted to annual maximum time series derived for 1976-2100.
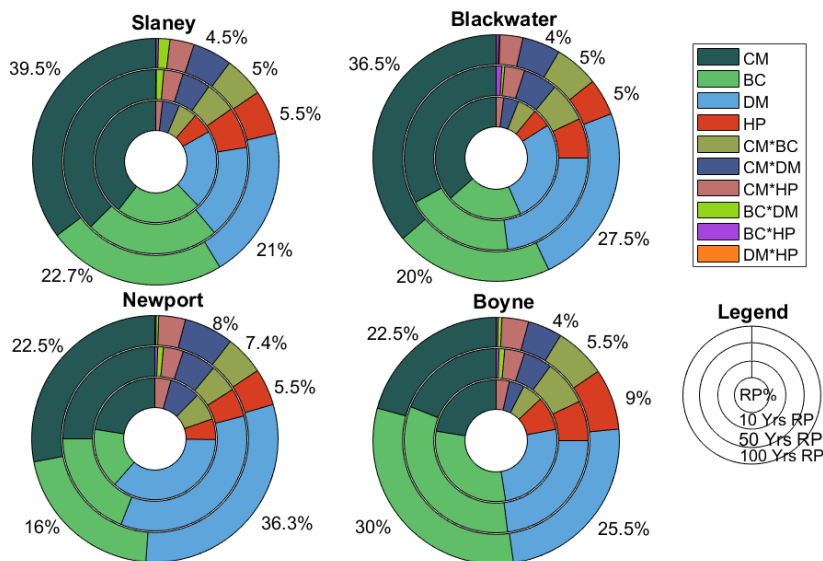
Figure 12. Contribution of each component of the modelling chain, together with their interaction, to the range of simulated changes in flood hazard magnitude for the 2080s (2070-2099) relative to the reference period (1976-2005). Sources considered include 12 CMIP6 climate models (CM), 5 bias correction techniques (BC), hydrological model parameter uncertainty (HP) and 3 extreme value distribution models (DM). The outermost circle/donut represents the flood quantile change at return period (RP) of 100 years, the middle circle RP of 50 years and innermost circle RP of 10 years for the 2080s. Percent changes are annotated for the outermost circle (100-year flood).

925

Table 1. Statistical and hydro-climatic characteristics of each study catchment.

	Boyne	Blackwater	Slaney	Newport
Latitude [degree]	53.60	52.14	52.80	53.95
Longitude [degree]	-6.96	-8.94	-6.61	-9.44
Catchment Area [km^2]	2447.36	1257.20	1032.68	146.02
Mean Elevation [m]	70.00	116.00	107.00	56.00
Mean of annual max precipitation [mm]	28.58	39.17	38.23	41.69
Mean of annual max streamflow [m^3/s]	232.22	233.59	137.39	24.26
lower quantile of precipitation (P85) [mm]	0.01	0.02	0.01	0.04
higher quantile of precipitation (P15) [mm]	5.46	8.25	6.60	9.95
Low flow (Q95) [m^3/s]	4.67	4.47	4.10	0.81
Peak flow (Q5) [m^3/s]	106.22	105.40	53.30	16.20
Coefficient of Variance of streamflow [-]	37.97	23.79	30.92	18.07
Coefficient of Variance of precipitation [-]	29.34	24.68	30.86	33.17
Base flow index [-]	0.72	0.62	0.73	0.69
Mean of surface runoff [m^3/s]	10.21	13.14	5.77	1.86
Mean of base flow [m^3/s]	26.85	21.78	15.58	4.19

930

935

940

945

Table 2 List of CMIP6 climate models employed in this study

Code	Institute	Parent source Id	Institution Id
CM1	Commonwealth Scientific and Industrial Research Organisation, Australia	ACCESS-CM2	CSIRO
CM2	Beijing Climate Center, China	BCC-CSM2-MR	BCC
CM3	National Center for Atmospheric Research, USA	CESM2	NCAR
CM4	European: EC-EARTH consortium	EC-Earth	EC-EARTH consortium
CM5	Global Fluid Dynamics Laboratory, USA	GFDL	NOAA-GFDL
CM6	Met Office Hadley Centre, UK	HadGEM3-GC31-LL	MOHC
CM7	JAMSTEC, AORI, NIES, and R-CCS, Japan	MIROC6	MIROC
CM8	Max Planck Institute for Meteorology, Germany	MPI-ESM1-2-HR	MPI-M
CM9	Meteorological Research Institute, Japan	MRI-ESM2-0	MRI
CM10	Nanjing University of Information Science and Technology, China	NESM3	NUIST
CM11	NorESM Climate modeling Consortium, Norway	NorESM2-LM	NCC
CM12	Met Office Hadley Centre, UK	UKESM1-0-LL	MOHC

950